INFECTION AND IMMUNITY, Nov. 2006, p. 6408–6418 Vol. 74, No. 11
0019-9567/06/$08.00+0 doi:10.1128/IAI.00538-06

Interaction of a Neurotropic Strain of *Borrelia turicatae* with the Cerebral Microcirculation System▽

Nilay Sethi,[1,2]† Marie Sondey,[1,2] Yunhong Bai,[1,2]‡ Kwang S. Kim,[3] and Diego Cadavid[1,2]*

Department of Neurology and Neuroscience[1] and Center for the Study of Emerging Pathogens,[2] University of Medicine and Dentistry of New Jersey-New Jersey Medical School, Newark, New Jersey 07103, and Pediatric Infectious Diseases, Johns Hopkins University School of Medicine, Baltimore, Maryland[3]

Received 3 April 2006/Returned for modification 10 May 2006/Accepted 14 August 2006

Relapsing fever (RF) is a spirochetal infection characterized by relapses of a febrile illness and spirochetemia due to the sequential appearance and disappearance of isogenic serotypes in the blood. The only difference between isogenic serotypes is the variable major outer membrane lipoprotein. In the absence of specific antibody, established serotypes cause persistent infection. Studies in our laboratory indicate that another consequence of serotype switching in RF is a change in neuroinvasiveness. As the next step to elucidate this phenomenon, we studied the interaction of the neurotropic Oz1 strain of the RF agent *Borrelia turicatae* with the cerebral microcirculation. During persistent infection of antibody-deficient mice, we found that serotype 1 entered the brain in larger numbers and caused more severe cerebral microgliosis than isogenic serotype 2. Microscopic examination revealed binding of *B. turicatae* to brain microvascular endothelial cells in vivo. In vitro we found that *B. turicatae* associated with brain microvascular endothelial cells (BMEC) significantly more than with fibroblasts or arachnoidal cells. The binding was completely eliminated by pretreatment of BMEC with proteinase K. Using transwell chambers with BMEC barriers, we found that serotype 1 crossed into the lower compartment significantly better than serotype 2. Heat killing significantly reduced BMEC crossing but not binding. We concluded that the interaction of *B. turicatae* with the cerebral microcirculation involves both binding and crossing brain microvascular endothelial cells, with significant differences among isogenic serotypes.

Infection of the central nervous system (CNS) is a characteristic feature of several pathogenic spirochetes, including the agent of syphilis, *Treponema pallidum*, and many of the *Borrelia* spp. that cause Lyme disease (LD) or relapsing fever (RF). RF is best known for antigenic variation due to spontaneous serotype switches by variable expression of immunodominant outer membrane lipoproteins, referred to as variable major proteins (VMP). The VMP switch allows RF borrelias to escape killing by the host's serotype-specific antibody response (1, 9, 19). In mice infected with the RF agents *Borrelia hermsii* strain HS1 (9) and *B. turicatae* strain Oz1 (12, 15), we have observed significant differences in the ability of isogenic serotypes to enter the brain. Since immunocompetent mice in most cases eliminate the predominant serotypes from blood and brain via production of VMP-specific antibodies, to be able to study CNS infection by specific serotypes over time we had to use B-cell-deficient mice. In mice with severe combined immunodeficiency (*scid*), which are B and T cell deficient, we isolated and characterized two isogenic serotypes of the Oz1 strain of *B. turicatae* of different virulence and CNS tropism: serotype 2 (formerly known as serotype B) is characterized by a VMP of 20 kDa, called Vsp2 for variable small protein 2, and serotype 1 (formerly known as serotype A) is characterized by a VMP of 23 kDa, called Vsp1. While serotype 2 was found to be more virulent, killing infant mice and causing more severe arthritis and carditis (13, 15, 40), serotype 1 was found to be more neurotropic, infecting the CNS five times more than serotype 2. More recently, we characterized a novel serotype, serotype 3, which turned out to be neurotropic in *scid* mice and caused residual brain infection in immunocompetent mice (14).

The neurological complications of borrelial infections are collectively referred to as neuroborreliosis (6). Our laboratory studies the pathogenesis of neuroborreliosis in nonhuman primates infected with LD borrelias (2, 7, 10, 39) and in mice infected with RF borrelias (9, 15). The studies of *scid* mice persistently infected with *B. turicatae* have shown that it rapidly infects the central nervous system (CNS) (12, 15). Although the preferred localization of RF and LD borrelias in the CNS is the subarachnoid space (2, 10, 12), the site of entry remains to be determined. Several studies in vitro have shown that spirochetes can move across endothelial cells intercellularly (18, 25) and that blood-brain barrier crossing in vivo may be done with the help of the host's proteases (17, 24, 38). There is also evidence that the presence of *Borrelia burgdorferi* in the circulation results in increased permeability of the blood-brain barrier (22). The present study characterized the interaction of a neurotropic spirochete, the Oz1 strain of *B. turicatae*, with the cerebral microcirculation. The results revealed an important association between *B. turicatae* and brain microvascular endothelial cells from both mice and humans. Significant differences were found in the ability of isogenic serotypes to cross

* Corresponding author. Mailing address: 185 South Orange Avenue, MSB H506, Newark, NJ 07103. Phone: (973) 972-8686. Fax: (973) 972-5059. E-mail: cadavidi@umdnj.edu.

† Present address: UMDNJ-Robert Wood Johnson Medical School, New Brunswick, N.J.

‡ Present address: Department of Neurology, Wayne State University School of Medicine, Detroit, MI 48201.

▽ Published ahead of print on 28 August 2006.

the blood-brain barrier in vivo and brain microvascular endothelial cell barriers in vitro.

MATERIALS AND METHODS

Strains and culture conditions. *B. turicatae* strain Oz1 and serotypes 1 and 2 (previously referred to as serotypes A and B, respectively) have been previously described (12, 13, 15, 40, 41). Serotype 3 was recently isolated from a mouse with residual brain infection (14). Borrelias were cultured in Barbour-Stoenner-Kelly-H (BSK-H) medium (4) and counted in a Petroff-Hauser chamber under phase-contrast microscopy (3). The purity of the borrelia populations was assessed by Western blotting with serotype-specific monoclonal antibodies 1H12 (for Vsp1) and 5F12 (for Vsp2) (13, 40). For transwell experiments (see below), borrelias were grown in BSK-H media at 34°C supplemented with 50 μCi ml^{-1} [^{35}S]methionine and [^{35}S]cysteine (Amersham). At late log phase, borrelias were pelleted by centrifugation at 13,000 $\times$ *g* for 20 min at room temperature, washed with BSK media three times to remove unbound radioactivity, resuspended in BSK-H media with 10% dimethyl sulfoxide at a concentration of 10^8 spirochetes/ml, aliquoted, stored frozen at −80°C, and used within 2 months. Precipitation with 20% trichloroacetic acid was used to confirm that the majority of the radioactivity in ^{35}S-labeled spirochetes was protein bound. Radiolabeled spirochetes were examined microscopically after thawing to confirm their viability.

Mouse infections. The housing and care of mice was in accordance with the Animal Welfare Act. Four-week-old female mice with severe combined immunodeficiency (*scid*) from Charles Rivers were inoculated intraperitoneally with 10^3 spirochetes in 200 μl of phosphate-buffered saline (PBS). *scid* mice were maintained in germ-free environments before and after infection. Two separate experiments were done, one for histological analysis and one for measurement of the spirochetal load by reverse transcription-PCR (RT-PCR). For each experiment, groups of four mice each were inoculated with serotype 1 or serotype 2 alone or in combination or with PBS as a control. Infection was confirmed by examining tail vein blood under phase-contrast microscopy. Necropsy was performed essentially as described previously (9), with an additional perfusion with 30 ml of 4% paraformaldehyde for mice used for histological analysis. Whole brains used for RT-PCR were rinsed twice with 0.5 ml of sterile PBS to further minimize blood contamination and frozen at −80°C for RNA extraction later on.

Immunohistochemistry and digital image analysis. Mouse heads were removed after peeling off the skin at necropsy, fixed in 4% paraformaldehyde for 48 h at 4°C, and decalcified in 20% EDTA for 3 weeks with weekly changes of solution. Immunohistochemistry for detection of spirochetes in the brain was performed essentially as described previously (12) using 0.5 mg/ml of protease type VIII (P-5380; Sigma) for antigen retrieval. Anti-Vsp1 monoclonal antibody 1H12 was used for detection of serotype 1 in brain (12). For measurement of brain inflammation, we used rat monoclonal antibody anti-mouse F4/80 (Serotec, United Kingdom) diluted 1/1,000. Goat anti-mouse NF-κB diluted 1/500 (#372; Santa Cruz) was used as a positive control in studies of macrophage activation in vitro. Tissue sections from uninfected animals were used as negative controls. Purified immunoglobulin G of the same species (Sigma) or nonrelevant primary antibodies matched for concentration and isotype were used as negative controls. Tissue sections were examined by light microscopy by a neuropathologist (D. Cadavid) masked to the infectious status. To measure cerebral microgliosis, we did digital image analysis of F4/80-stained coronal brain sections using Image Pro Plus Software (Media Cybernetics, MD). A masked examiner (Y. Bai) photographed four or more 20× microscopic fields per mouse. Results are given as the mean (95% confidence interval) sum area in square microns per 40× microscopic field.

TaqMan RT-PCR. TaqMan RT-PCR for quantification of *B. turicatae* was performed essentially as described previously (2, 7). Total RNA was extracted with Trizol reagent (Life Technologies) from whole-perfused brains that had been homogenized with the Fastprep system (Savant). The reverse transcription (RT) was performed in 20-μl reaction volumes. One microgram of total RNA was used as template for each RT. For preparation of the standard curve, cultured borrelias were counted in a Petroff-Hausser chamber by phase-contrast microscopy, and RNA was extracted from $\log_{10}$ dilutions of known numbers of spirochetes. A preliminary comparison of separate standard curves using $\log_{10}$ dilutions of spirochetes grown in vitro or spirochetes grown in vivo (necropsy plasma) showed similar results, validating the use of cultured spirochetes for the standard curve (data not shown). PCRs with H_20 instead of cDNA were included as negative controls. To control for the amount of host input RNA, we used TaqMan RT-PCR of mouse 18S rRNA with commercially available primers and probe (4319413E; Applied Biosystems). Serial dilutions of known amounts of mouse 18S cDNA were used as positive controls for the standard curve.

Cell culture. Five different cell lines were used for the cell culture studies. The mouse J774 monocytic cell line was grown in RPMI medium (Sigma) with 10% fetal bovine serum. For transwell assays, four different human cell lines were used: brain-microvascular endothelial cells (BMEC) (37), fibroblasts (IMR90) (29) transformed with simian virus 40 (SV40), F5 meningioma (arachnoidal) cells, and CACO2 colonic carcinoma cells (ATCC HTB37). These cell lines were grown at 37°C and 5% CO_2 in media with 10% fetal bovine serum. IMR90 medium was 1:1 Dulbecco's modified Eagle's medium (DMEM)/F10; F5 medium was RPMI; BMEC medium was RPMI, 10% NuSerum, minimal essential medium (MEM) vitamins, MEM nonessential amino acids, 1 mM sodium pyruvate, 2 mM L-glutamine, 30 μg/ml endothelial growth supplement, and 5 U/ml heparin; and CACO2 medium was DMEM with L-glutamine and nonessential amino acids. Clear DMEM (D1145; Sigma) was used for all experiments involving 2000 dextran blue. Preliminary experiments showed that *B. turicatae* remained viable on BMEC, IMR, and F5 media for up to 24 h, while none of the eukaryotic cell lines grew well in BSK media. Therefore, all in vitro assays were done in eukaryotic cell media.

Immunofluorescence. BMEC were grown to confluence on four-chamber glass slides (Falcon). Serotype 1 (8×10^6 cells/well in a 200-μl volume) was incubated with BMEC monolayers for 1 to 2 h at 37°C, followed by rinsing three times in buffer to remove unbound spirochetes and fixing with 100% ethanol for 10 min. This was followed by staining of BMEC with 1,1′-di-octadecyl-3,3,3′,3′-tetramethylindocarbocyanide perchlorate (DiI; Molecular Probes) for 20 min and immunostaining of bound spirochetes or their products with αVsp1 rabbit antiserum diluted 1:1,000 for 30 min, followed by incubation with goat polyclonal anti-rabbit fluorescein isothiocyanate (FITC) conjugate diluted 1:100 for 30 min. Slides were washed with Optimax buffer (Biogenex) three times between all incubations. Vectashield antifading agent (Vector) was used to examine slides by fluorescence microscopy with FITC, rhodamine, or dual FITC/rhodamine filters (Olympus).

Transwell assays. Cells were released from culture flasks by trypsinization, resuspended in fresh media, and counted by phase-contrast microscopy with a hemocytometer after mixing with trypan blue to examine viability. Two types of transwell chambers were used: large and small. For large transwells, 5×10^5 eukaryotic cells were seeded in the upper chamber in 500 to 600 μl of media, and 1,000 to 1,500 μl of media was added to the lower chamber. The larger transwells were Corning Incorporated Costar 3493, which are collagen coated, 12 mm in diameter, 3.0 μm in pore size, and placed in 12-well culture plates (3513; Corning Costar). The smaller transwells were identical to the larger ones but were 6.5 mm in diameter (3496; Costar) and seeded with 2×10^5 cells, and the volumes in the upper and lower chambers were smaller: 100 and 600 μl, respectively. The cells were grown on the chambers for 1 to 3 days. A total of 5×10^3 to 5×10^4 counts per minute (cpm) of radiolabeled live or heat-killed borrelias, corresponding to 1×10^6 to 1×10^7 spirochetes, were added to the upper chamber. Phase-contrast microscopic examination of radioactive samples from the upper and lower chambers at different times revealed that the measurement of radioactivity corresponded to the presence of viable spirochetes (data not shown). The viability of frozen radioactive borrelia stocks after thawing in eukaryotic cell media was greater than 90%. The smaller transwells were used for single-time-point assays, and the larger transwells were used for multiple-time-point assays. Therefore, the results from the smaller transwells were direct measurements of radioactivity, while the results from the larger transwells were estimates based on 20-μl samples removed from the upper and lower chambers at various times and counted in scintillation cocktails. For the smaller transwells, the BMEC monolayer was cut from the plastic inserts with a disposable blade and similarly counted in scintillation cocktails. All transwell assays were done in triplicate. In select experiments, BMEC transwells were pretreated with 200 mU of proteinase K (Sigma) for 1 h, washed three times with fresh media, and examined for confluence by phase-contrast microscopy prior to use. The barrier function of BMEC monolayers was measured by adding 50 mg of 2000 dextran blue (Sigma) diluted in DMEM clear media to the upper chamber of transwells and measuring the optical density by spectrophotometry in aliquots removed from the lower chambers at various times. A standard curve with serial dilutions of known amounts of dextran blue was used for quantitation. The electrical resistance across the monolayers was measured with an epithelial voltohmmeter (catalog no. 070601; WPI) using the STX2 electrode (no. 062901; WPI) according to the manufacturer's instructions.

Statistical analysis. Comparisons of barrier crossing and binding at multiple time points were performed using two- and three-way factorial analysis of variance models. *P* values for multiple comparisons were evaluated using Sidak's adjustment. Comparisons of single time points used two-sided *t* tests for samples of equal variance. *P* values of less than 0.05 were considered significant.

TABLE 1. Infection and inflammation in the brain of *scid* mice 1 month after inoculation with *B. turicatae*

Inoculum	Mean spirochetes per μg of brain RNA[a] (95% CI)	Sum area stained for F4/80[b] (95% CI)
Serotype 1	40 (26–67)	33,000 (23,000–43,000)
Serotype 2	4 (2–6)	4,900 (3,300–6,500)
PBS	0	1,200 (300–1,200)

[a] Results were measured by TaqMan RT-PCR amplification of 16S rRNA. $P < 0.001$ for the difference between serotypes 1 and 2.

[b] Results are mean (95% confidence interval) sum areas in square microns per 40× microscopic field. $P < 0.001$ for the differences between serotype 1 and PBS as well as serotype 1 and serotype 2; $P < 0.05$ for the difference between serotype 2 and PBS. Activated macrophages/microglia were detected by immunostaining with rat anti-mouse F4/80 monoclonal antibody.

RESULTS

***Borrelia turicatae* causes brain infection in mice.** Previous studies in mice inoculated with the Oz1 strain of *B. turicatae* using culture in BSK-II media (15) or immunohistochemistry (12) showed CNS infection occurs early on and varies in severity, depending on the infecting serotype. To better measure the differences in CNS infection between isogenic serotypes of *B. turicatae*, we did TaqMan RT-PCR amplification of the 16S rRNA of *Borrelia* spp. in whole-brain RNA 1 month after inoculation of *scid* mice with 10^3 spirochetes of serotype 1 (serotype 1) or serotype 2 (serotype 2) alone or in combination. We have used this technique before successfully to measure the pathogen load in nonhuman primates infected with *B. burgdorferi* (2, 7, 39). *scid* mice inoculated with PBS were used as a control. This study could not be done in immunocompetent mice, because they clear serotype 1 and serotype 2 from the blood within 5 days (9). Western blotting of plasma cultures 1 month after inoculation showed that all mice inoculated with *B. turicatae* developed persistent infection with the serotypes with which they were originally inoculated (data not shown). TaqMan RT-PCR of borrelia 16S rRNA showed the brains of mice infected with serotype 1 had 10 times more spirochetes than the mice infected with serotype 2 (Table 1). *scid* mice infected with a 1:1 mixture of serotypes 1 and 2 had a mean number of spirochetes and 95% confidence interval (95% CI) in the brain that was intermediate between mice infected with either serotype alone: 16 (95% CI, 10 to 21). Even after adjusting for the amount of input mRNA using TaqMan RT-PCR of mouse 18S rRNA, we found significantly more serotype 1 than serotype 2 in the brain: the mean (95% confidence intervals) number of spirochetes per microgram of 18S cDNA was 30 (15 to 52) and 7 (4 to 10) with serotype 1 and serotype 2, respectively ($P = 0.03$). We concluded that *B. turicatae* causes persistent brain infection in *scid* mice to different degrees depending on the infecting serotype.

Cerebral microgliosis in mice persistently infected with *B. turicatae*. To investigate whether brain infection with *B. turicatae* resulted in CNS inflammation, we inoculated new groups of four *scid* mice each with serotype 1, serotype 2, or PBS and measured cerebral microgliosis in perfused brains 1 month later. Cerebral microgliosis was chosen because others have shown it is a prominent feature of brain inflammation with *B. turicatae* (35). Furthermore, previously we showed hematoxylin and eosin staining did not reveal any inflammation in the brain parenchyma of *B. turicatae*-infected mice (12, 14). For this, we used a monoclonal antibody to the murine macrophage cell surface glycoprotein F4/80, a well-established marker of activated murine macrophages/microglia (42). F4/80-positive cells were only rarely observed in brains from uninfected controls and were mostly perivascular (Fig. 1B and D). In contrast, mice infected with serotype 1 had widespread and severe cerebral microgliosis (Fig. 1A and C). Microgliosis was less apparent in mice infected with serotype 2 (Fig. 1E and F). Digital image analysis of F4/80 immunostaining showed there was nearly 30 times more F4/80 staining per 40× microscopic field in serotype 1-infected mice than in uninfected controls ($P < 0.001$) (Table 1). F4/80 immunostaining was also increased in serotype 2-infected mice compared to uninfected controls, but this was significantly less than with serotype 1 ($P < 0.001$) (Table 1).

F4/80-positive cells in infected mouse brains had heterogeneous morphology, with some appearing ameboid and others ramified (Fig. 1). Some argue that ramified morphology is evidence of a resting stage (44). However, it has been shown that F4/80 is a marker of activated microglia (42), and some argue that ramified microglial morphology is not inconsistent with an activated state (26). To clarify whether F4/80 is a valid marker of borrelial microglial activation, we did F4/80 immunostaining in a mouse monocytic cell line (J774). For this, we grew J774 cells on culture slides in the presence of 10^6 serotype 1 spirochetes/ml of serum-free DMEM or media alone as a control and examined them by immunostaining for F4/80 and NF-κB as a positive control. NF-κB is a well-known transcription factor produced in response to lipoprotein activation of macrophages via TLR2 (30). Digital image analysis of immunostained slides showed that the mean (95% CI) sum area (in micrometers squared) positive for F4/80 per 40× microscopic field was 1×10^5 (5.6×10^4 to 1.55×10^5) and 3×10^3 (8×10^2 to 5.3×10^3) for incubation with serotype 1 or media alone, respectively. The corresponding values for NF-κB were 1.47×10^5 (1×10^5 to 1.83×10^6) and 5×10^3 (0 to 1×10^4). The differences between serotype 1 and media were statistically significant for both F4/80 and NF-κB ($P < 0.001$). Since F4/80 staining was very low in unstimulated monocytes but increased 100-fold after incubation with serotype 1, very similar to NF-κB, we concluded that F4/80 is a valid marker of monocyte activation in response to borrelia stimulation.

Interaction of *B. turicatae* with brain microvascular endothelial cells in vivo. The previous results showed that *B. turicatae* caused persistent CNS infection and microgliosis in *scid* mice and that it did so to different degree depending on the infecting serotypes. To investigate whether this resulted from differences in the interaction of isogenic serotypes with the cerebral microcirculation, we studied the localization of spirochetes in perfused brains from *scid* mice persistently infected with serotype 1 or serotype 2. Light microscopic examination of coronal sections immunostained with monoclonal antibody αVsp1 or αVsp2 confirmed the previous observation that the localization of serotype 1 and serotype 2 in the CNS is primarily subarachnoidal (Fig. 2A) (12). However, examination of the cerebral microcirculation revealed frequent spirochetes that appear in physical contact with endothelial cells in mice infected with either serotype, more often in leptomeningeal vessels (Fig. 2B) but also occasionally in brain parenchymal ves-

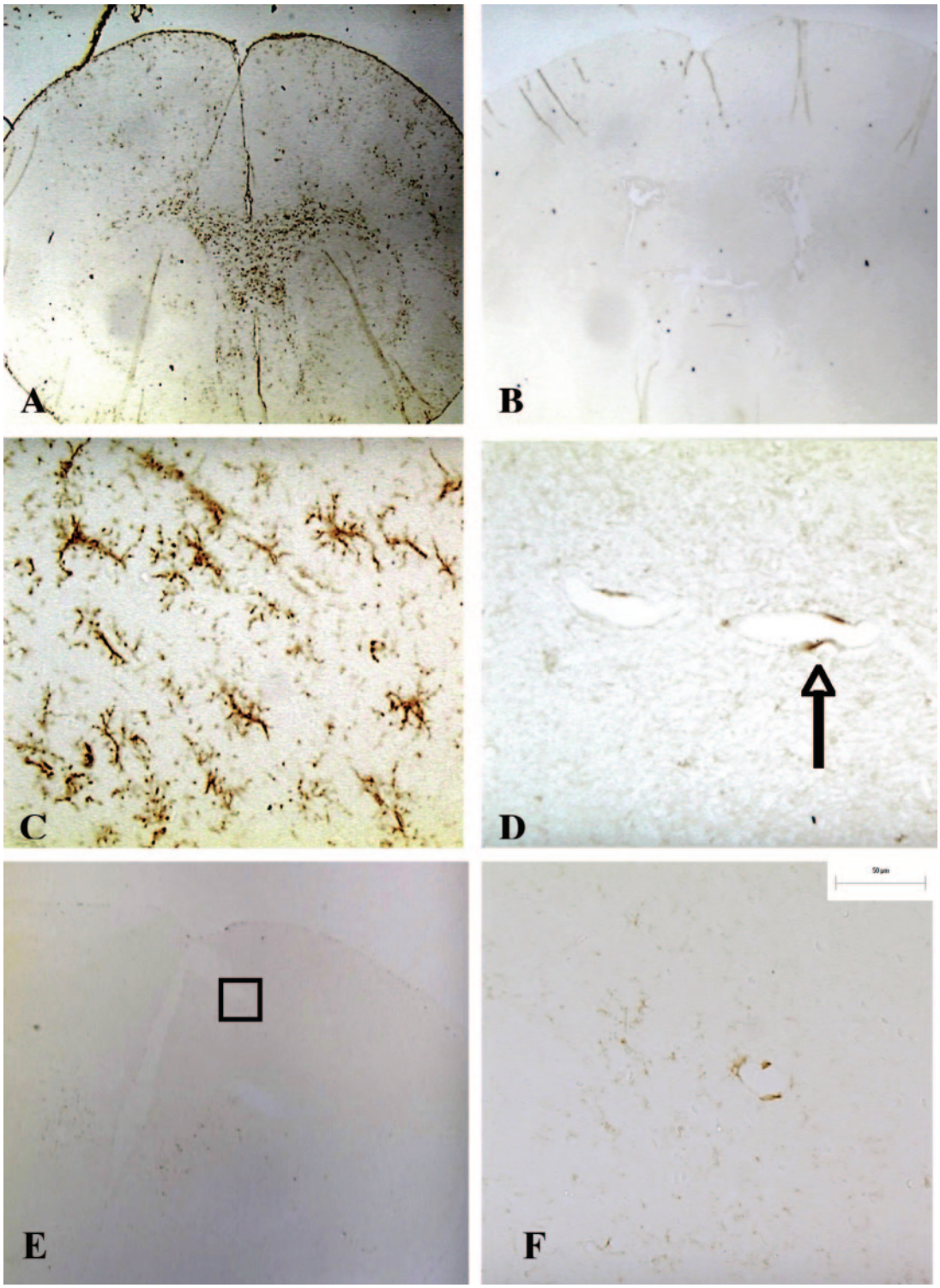

FIG. 1. Cerebral microgliosis in *scid* mice persistently infected with serotype 1 of *B. turicatae*. Immunostaining with rat anti-mouse F4/80 monoclonal antibody shows extensive microgliosis in the brain of a *scid* mouse persistently infected with serotype 1 of *B. turicatae* (A). In comparison, little staining is seen in an uninfected control (B) or in a *scid* mouse persistently infected with serotype 2 (E) (magnification, ×20). Selected areas of the cerebral cortex (shown in squares in panels A, B, and E) are shown at higher magnifications in panels C, D, and F, respectively (×400). The arrow in panel D points to a perivascular F4/80-positive cell.

sels (Fig. 1C). Some spirochetes appeared to be crossing leptomeningeal endothelial cells (Fig. 2D) to reach the subarachnoid space (Fig. 2A). However, whether there were more serotype 1 than serotype 2 spirochetes crossing leptomeningeal endothelial cells could not be determined. These results support the view that CNS infection by *B. turicatae* involves binding to brain microvascular endothelial cells, preferentially in the leptomeningeal microcirculation followed by crossing of

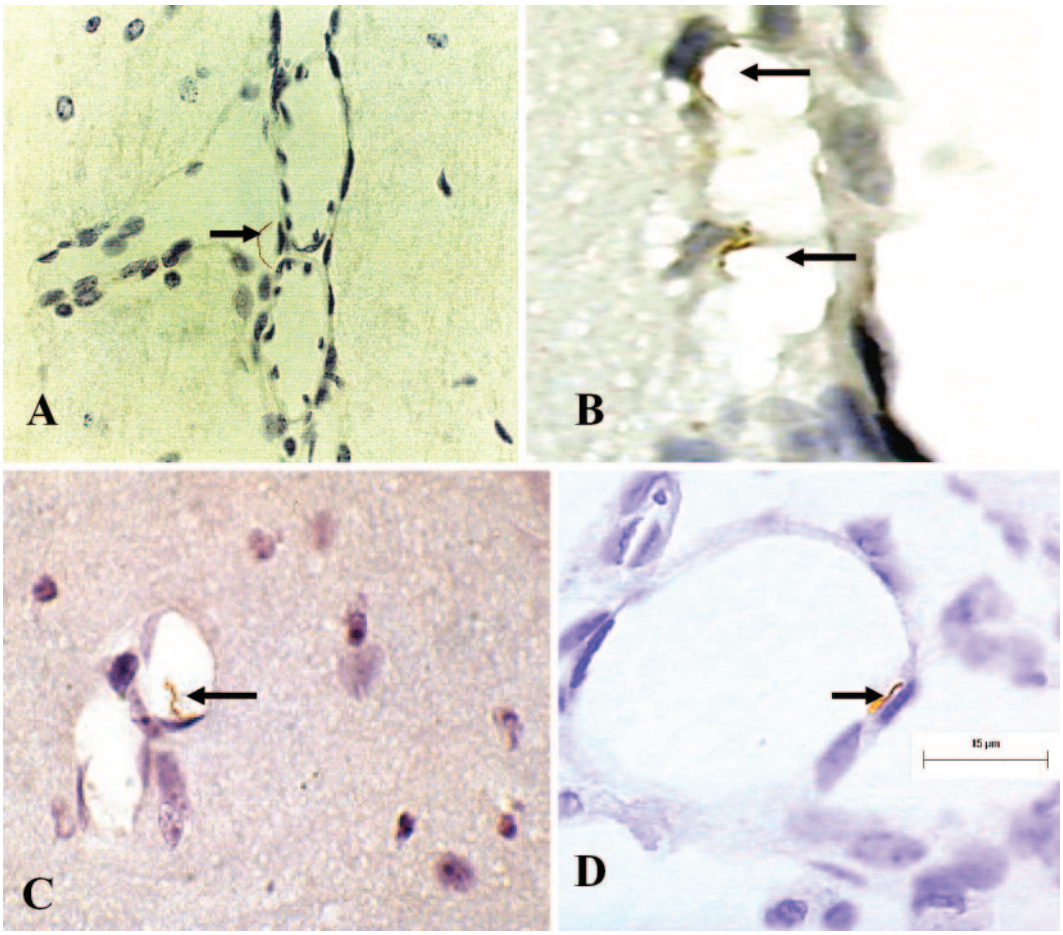

FIG. 2. Interaction of *B. turicatae* with cerebral microcirculation in vivo. Immunostaining with αVsp1 monoclonal antibody 1H12 of *scid* mouse brains 1 month after intraperitoneal inoculation with serotype 1 of *B. turicatae* is shown. Arrows point to spirochetes on the abluminal side of the leptomeningeal microcirculation within the subarachnoid space (A), bound to the luminal side of leptomeningeal cells (B), bound to brain parenchymal endothelial cells (C), and in the process of crossing leptomeningeal endothelial cells (D). 3,3′-Diaminobenzidine chromogen staining; magnification, ×1,000.

the blood-brain barrier. However, we were not able to determine whether it occurs intracellularly, intercellularly, or both.

Interaction of *B. turicatae* with brain microvascular endothelial cells in vitro. The previous studies revealed an important interaction does take place between *B. turicatae* and the cerebral microcirculation in vivo. To further investigate this, we studied the interaction of *B. turicatae* with brain microvascular endothelial cells in vitro. For this we used serotype 1 of *B. turicatae* (serotype 1) and an SV40-transformed human brain microvascular endothelial cell line that has proved useful in other studies of neurotropic bacteria (37). First, we studied whether serotype 1 associates with BMEC by double immunofluorescence microscopy. BMEC grown on cell culture slides were incubated with serotype 1 spirochetes at 37°C and, after rinsing with buffer, labeled with the fluorescent dye DiI that labels BMEC cytoplasmic membranes with an orange color. Bound spirochetes or their outer membrane fragments were visualized by immunostaining with a rabbit polyclonal antibody to Vsp1, the major outer membrane lipoprotein of serotype 1, followed by an FITC-labeled secondary antibody. The results (Fig. 3) showed FITC (green) signal corresponding to Vsp1 in spirochetes that appear bound to DiI-labeled (orange) BMEC membranes. Several areas of yellow color seen at the interface between spirochetes and BMEC indicate colocalization of Vsp1 (FITC) and BMEC cytoplasmic membranes (DiI). However, FITC signal without spiral morphology was also observed and appeared to be in the cytoplasm of BMEC (arrow in Fig. 3). Since BMEC were extensively rinsed with buffer after incubation with serotype 1 and prior to immunostaining, this amorphous FITC signal is unlikely to be extracellular. They also do not appear to be membrane bound due to the absence of yellow color. We concluded that serotype 1 binds to BMEC membranes.

Our studies of the localization of *B. turicatae* in *scid* mice had also revealed important associations with fibroblasts in the duramater and arachnoidal cells in the leptomeninges (12). Therefore, we studied the association of *B. turicatae* with BMEC in comparison with fibroblasts and arachnoidal cells, the main components of the duramater and arachnoid, respectively. We used IMR90, an SV40-transformed human lung

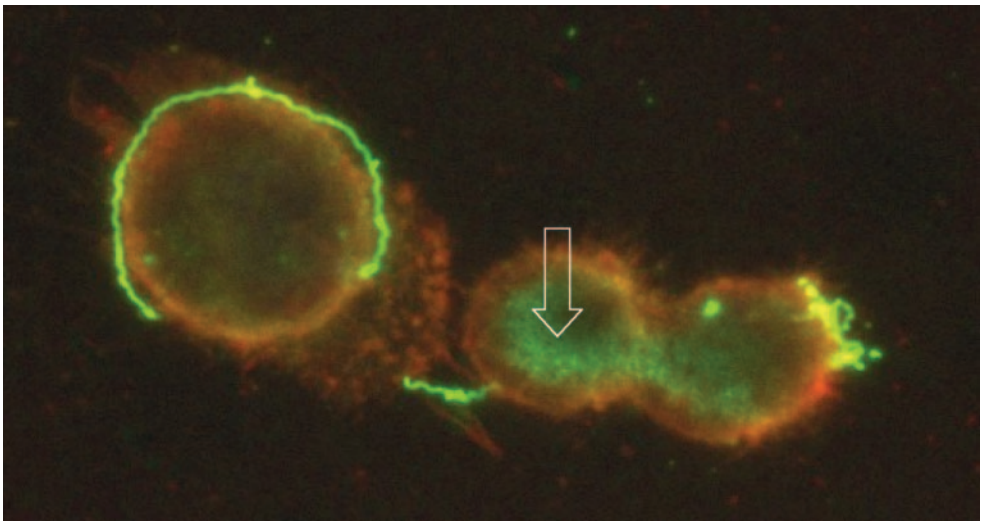

FIG. 3. Interaction of serotype 1 of *B. turicatae* with brain microvascular endothelial cells (BMEC) in vitro. BMEC grown on cell culture slides were incubated with serotype 1 spirochetes, washed, incubated with DiI to label BMEC membranes orange, and immunostained with αVsp1 monoclonal antibody 1H12, followed by an FITC-labeled secondary antibody to label Vsp1 green. Microscopic examination with a dual FITC and rhodamine filter revealed green spirochetes next to BMEC. The spirochetes on the surface of BMEC show areas of yellow color, representing colocalization of Vsp1 and BMEC cytoplasmic membrane. Green signal, representing Vsp1, is seen not only extracellularly in spirochetes but also inside BMEC as amorphous material (open white arrow) (magnification, ×1,000).

fibroblast cell line, and F5, a human arachnoidal cell line isolated from a patient with meningioma. To compare the binding of these cells to serotype 1, we used radiolabeling of spirochetes. For this, we added 2×10^4 counts per minute (cpm) of radiolabeled serotype 1 spirochetes to transwell chambers with confluent monolayers of BMEC, IMR90, or F5 cells and measured the radioactivity of the fluid from the upper and lower chambers and the monolayer after a single time interval. All assays were done in triplicate and repeated at least twice for consistency. We verified in aliquots from the upper and lower chamber examined by phase-contrast microscopy that spirochetes found in both the upper and lower chambers were viable. The results (Fig. 4) showed that the percentage of radioactivity associated with the monolayer was significantly higher with BMEC than with IMR90 or F5 cells: the mean (standard deviations [SD]) percentage of radioactivity in the monolayer after 24 h was 30.9 (8.7), 2.5 (0.4), and 2.6 (0.6) for BMEC, IMR90, and F5, respectively ($P < 0.001$ for the differences between BMEC and IMR or F5). We concluded that serotype 1 associated with BMEC significantly more than with IMR90 or F5 cells.

Pretreatment with proteinase K eliminates the association of serotype 1 with BMEC. The previous experiments revealed significant binding of serotype 1 to BMEC. We used digestion with proteinase K to investigate whether surface-exposed proteins mediate the binding of BMEC to serotype 1. For this, confluent monolayers of BMEC were treated with proteinase K or media alone as a control. After extensive rinsing with media, radiolabeled serotype 1 spirochetes were added to the upper compartment of transwell chambers. At three different times after inoculation, we removed samples from the upper and lower compartments and calculated the percentage of the total radioactivity found on the upper and lower compartments and the monolayer at each time point. The results showed that in untreated transwells the mean (SD) percentage of radioactivity associated with the BMEC monolayer increased over time from 16 (8.7) at 3 h to 30 (1.8) at 24 h (Fig. 5A). In contrast, pretreatment with proteinase K completely eliminated the association of serotype 1 with BMEC at all time points (Fig. 5B). As a result, the mean (SD) percentage of radioactivity found in the lower chamber at 24 h significantly increased from 15.6 (3.2) in untreated BMEC to 54.9 (5.7) in treated BMEC ($P < 0.001$). Unlike binding to serotype 1,

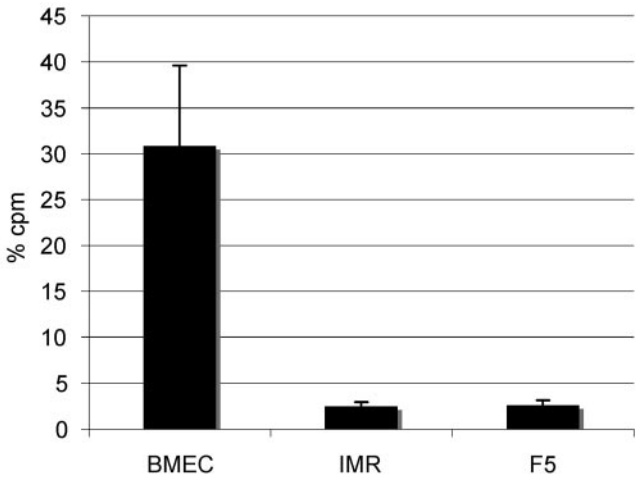

FIG. 4. Association of serotype 1 of *B. turicatae* with human brain microvascular endothelial, fibroblast, and arachnoidal cells. The association of serotype 1 of *B. turicatae* with human brain microvascular endothelial cells (BMEC), fibroblasts (IMR90), and arachnoidal cells (F5) was studied by measuring the radioactivity in the upper and lower chambers and the monolayer of smaller (6-mm) transwell chambers 24 h after inoculation of ^{35}S-labeled serotype 1 spirochetes in the upper chamber. The results are expressed as means (SD) of three to four separate transwells. Significant association of serotype 1 with the monolayers was observed only with BMEC ($P < 0.001$).

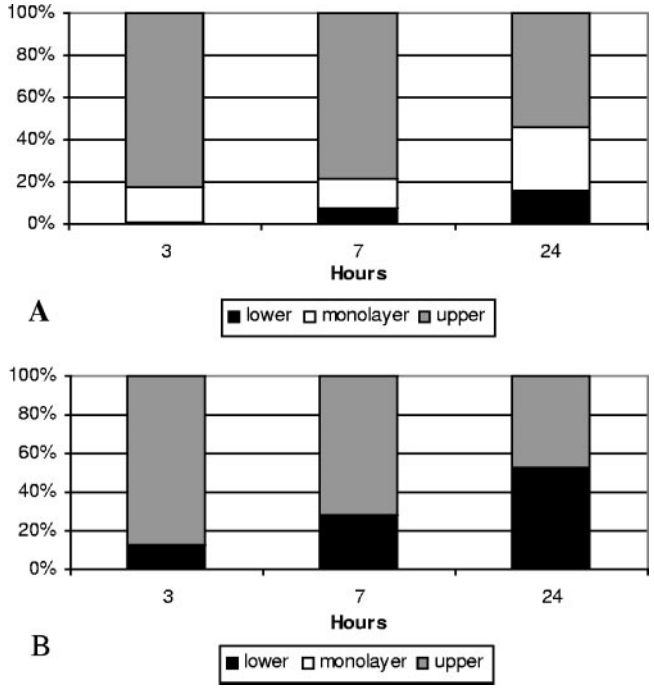

FIG. 5. Protease pretreatment eliminates the association of serotype 1 with brain microvascular endothelial cells. (A) Distribution of radioactivity in the three compartments (upper, monolayer, and lower) of large (12-mm) transwell chambers with BMEC barriers inoculated with serotype 1, shown as mean of $n = 3$ replicates. The mean (SD) percentage of radioactivity associated with the BMEC monolayer was 16 (8.7), 14 (5.3), and 30 (1.8) after 3, 7, and 24 h of incubation, respectively. (B) The effects of pretreating the BMEC monolayer with proteinase K are shown, illustrating that pretreatment completely eliminated the association with serotype 1 even after 24 h of incubation.

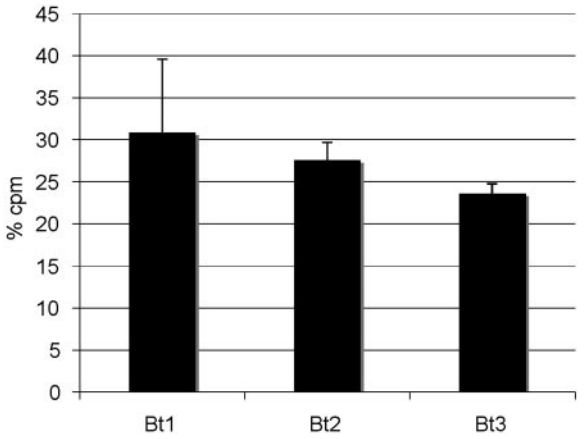

FIG. 6. Association of isogenic serotypes of *B. turicatae* with BMEC. Percentage of radioactivity associated with BMEC monolayers on transwell chambers 20 h after inoculation of ^{35}S-labeled serotypes 1 (Bt1), 2 (Bt2), and 3 (Bt3) of *B. turicatae* in the upper compartment. Results are expressed as means (SD) of three to four transwells each. Similar association with BMEC monolayers was observed with all serotypes tested (*P*, not significant).

pretreatment with proteinase K did not affect the barrier function of the BMEC monolayers measured by the crossing of 2000 dextran blue to the lower compartment (data not shown). Further evidence that pretreatment with proteinase K did not affect BMEC viability was the finding that incubation of BMEC with proteinase K for up to 4 h did not affect cell viability by trypan blue exclusion (data not shown). Therefore, we concluded that loss of cell surface proteins by proteinase K digestion completely eliminated the association of BMEC with serotype 1.

Comparison of the binding of isogenic serotypes of *B. turicatae* 224920 to BMEC. The previous results in vivo and in vitro revealed significant binding between *B. turicatae* and brain microvascular endothelial cells in vivo and in vitro. However, in vivo, even though serotype 1 caused greater CNS infection than serotype 2, both appeared to bind to leptomeningeal endothelial cells (Fig. 2). To investigate this further, we compared the binding of three different isogenic serotypes of *B. turicatae* to BMEC monolayers: serotype 1, serotype 2, and serotype 3. This and previous published studies have shown that although all three serotypes are capable of infecting the brain, at least one of them (serotype 2) does it to a much lesser degree (12, 14, 15). For this study, we used smaller (6-mm) transwells with confluent monolayers of BMEC cells inoculated with 2×10^4 cpm of radiolabeled spirochetes of each serotype. The radioactivity associated with the monolayer was directly measured 20 h later. The results showed that all three serotypes showed significant but similar binding to BMEC (Fig. 6). The mean (SD) percentage of radioactivity associated with BMEC was 30.8 (8.7), 27.6 (2), and 23.6 (1.1) for serotype 1, serotype 2, and serotype 3, respectively (*P*, not significant). We concluded that all three serotypes showed similar binding to BMEC.

Barrier function of BMEC monolayers. The previous study showed that the differences in neuroinvasiveness between serotype 1 and serotype 2 could not exclusively be explained by different binding to brain endothelial cells. Therefore, it became more likely that different ability to move across the blood-brain barrier may be the reason for the different neuroinvasiveness of *B. turicatae* serotypes. Since this could not be studied in vivo, we proceeded to study it in vitro using monolayers of human brain microvascular endothelial cells (BMEC). First, we determined the barrier function of BMEC monolayers by measuring the crossing of 2000 dextran blue from the upper to the lower chamber of small (6.5 mm) and large (12 mm) transwell chambers. Since dextran blue has a molecular weight of 2,000 Da, or 3.34×10^{-6} pg per molecule, we estimated that one molecule of 2000 dextran blue was about 12 times smaller than one molecule of Vsp1, which is 23 kDa. Therefore, blocking of 2000 dextran blue will indicate that BMEC were very likely to block whole spirochetes, outer membrane blebs or fragments, and even Vsp1 dimers. The results showed that 4 h after inoculation in the upper chamber, 80% of the 2000 dextran blue had reached the lower chamber when collagen-coated, polycarbonate membranes without any BMEC cells were used. In contrast, the mean (SD) percentage of 2000 dextran blue in the lower chamber was significantly reduced by BMEC monolayers to 10 (3) ($P < 0.001$). In comparison, IMR90 monolayers reduced the crossing to 15% (4%), while F5 and CACO2 monolayers reduced it to 37% (11%) and 37% (22%), respectively. To study the effect of the cell barriers on spirochetal crossing, we counted spirochetes in

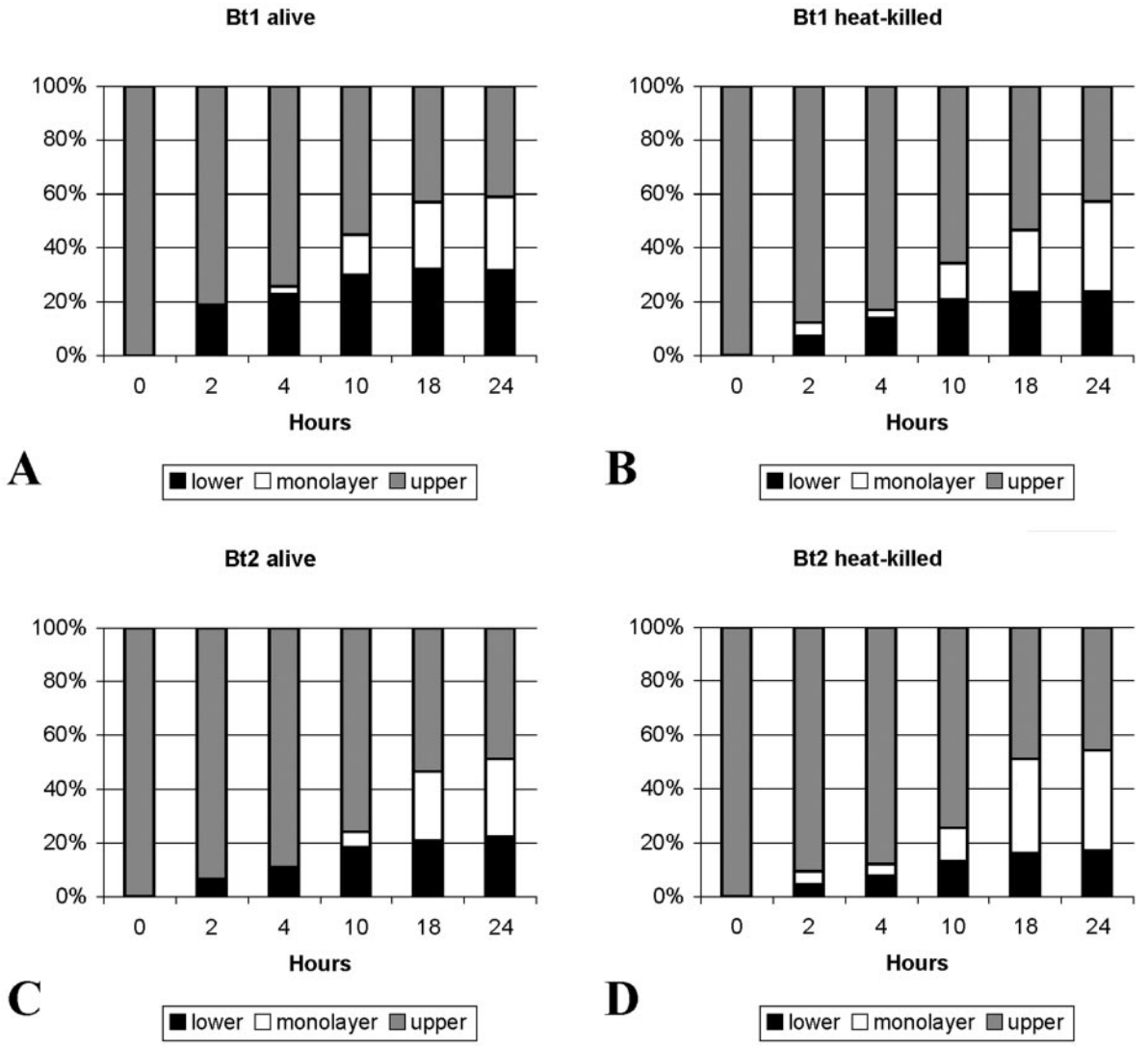

FIG. 7. Crossing of BMEC barriers by isogenic serotypes 1 and 2 of *B. turicatae*. Percentage (mean) of radioactivity in the three compartments (upper, monolayer, lower) of large (12-mm) transwell chambers with BMEC barriers inoculated with 1×10^7 radiolabeled serotype 1 (Bt1) or serotype 2 (Bt2) spirochetes alive (A and C) or heat-killed (B and D) are shown. All percentages are estimates based on measuring the radioactivity of 20-μl samples removed from the upper and lower chambers at each time point. Serotype 1 alive crossed into the lower chamber significantly better than serotype 2 alive ($P < 0.01$ by one-way analysis of variance for all time points). Heat killing significantly reduced the crossing into the lower chamber ($P < 0.01$ by *t* test). However, heat killing had no effect on binding to the BMEC monolayers.

the lower chambers of transwells with or without IMR90 monolayers after inoculation of serotype 1 into the upper chamber. The results showed that the IMR90 monolayers reduced the number of spirochetes reaching the lower chamber by 50 times at 3 h and by 20 times at 7 h (data not shown). Unlike the marked barrier effects found with dextran blue and spirochetal counting, measurement of electrical resistance across the monolayers with a voltohmmeter showed that the transepithelial/endothelial resistance (TEER) was only marginally increased by BMEC monolayers. The mean (SD) peak TEER of confluent BMEC was 113 (14) ohms/cm^2. This was lower than the mean (SD) TEER obtained with CaCO2 monolayers, 287 (26), and was only marginally increased compared with the negative control empty insert, which gave TEER readings of 94 (31) ohms/cm^2. In comparison, the TEER for the manufacturer-provided positive control inserts was 656 Ω (216 Ω/cm^2). These results are in agreement with previous measurements of TEER with BMEC (25). We concluded that BMEC monolayers, despite having low TEER, form a good physical barrier to the passive movement of even small particles.

Crossing of BMEC barriers by isogenic serotypes 1 and 2. In a previous study we had shown that serotype 1 moved across human umbilical endothelial cell monolayers better than serotype 2 (15). However, whether this was also the case for barriers of brain endothelial cells was not known. To investigate this, we measured the movement of serotype 1 and serotype 2 across BMEC monolayers grown on collagen-coated transwell chambers. BMEC grown on the larger (12-mm) transwells were chosen to be able to measure the movement at various times after inoculation. A total of 1×10^7 radiolabeled spiro-

chetes were inoculated into each of the upper chambers at time zero. Heat-killed spirochetes of both serotypes were also included to study the role of spirochetal viability in binding and crossing of BMEC barriers. The percentage of radioactivity in the three compartments at each time point was an estimate based on radioactive measurement of 20-μl aliquots removed from the upper and lower compartments at each time point, as depicted in Fig. 3. For clarity of presentation, we graphed the results as mean percentages of radioactivity for each compartment at each time point (Fig. 7). Figure 7A shows the results for live spirochetes, and Fig. 7B shows the results for heat-killed spirochetes. The results showed that, at all time points tested starting 4 h after inoculation, serotype 1 alive crossed into the lower chamber significantly better than serotype 2 alive ($P < 0.01$; adjusted for multiple comparisons). The estimated mean (SD) percentage of radioactivity in the lower chamber 2, 4, and 10 h after inoculation of serotype 1 alive was 20.3 (1.2), 25.4 (0.6), and 34.1 (1.5), compared to 7 (1.1), 11.8 (1.9), and 19.3 (1.9) with serotype 2 alive ($P < 0.01$ for each pair comparison by *t* test). Heat killing (Fig. 7B) significantly reduced the crossing of serotype 1 into the lower chamber to 7.7% (4.3%), 14.9% (6.4%), and 22.5% (5.3%) after 2, 4, and 10 h, respectively ($P < 0.01$ for all three comparisons by *t* test). In contrast, the only difference found in the association of serotype 1 and serotype 2 to the BMEC monolayer was that it started earlier for serotype 1 ($P < 0.05$ for the comparison at 10 h). Unlike crossing, heat killing did not affect association with the monolayer. However, the radioactivity from heat-killed serotype 1 accumulated into the lower chamber significantly better than from heat-killed serotype 2 at 10, 18, and 24 h ($P < 0.05$, adjusted for multiple comparisons). Microscopic examination of the upper and lower chambers from all transwells revealed motile spirochetes in all samples from transwells inoculated with live spirochetes (Fig. 7A). However, samples removed from the lower chambers inoculated with heat-killed borrelias did not have visible spirochetes but rather had only particles of amorphous material. This suggested that small fragments released by heat killing rather than intact but not viable spirochetes can cross BMEC barriers. We concluded that serotype 1 moves across BMEC barriers significantly better than serotype 2.

DISCUSSION

The limited number of bacteria able to cross the CNS barriers suggests they have very specific attributes. All neurotropic bacteria are invasive pathogens that multiply extracellularly, causing bacteremia, or multiply intracellularly within macrophages. Intracellular bacterial pathogens enter the CNS by using macrophages as "Trojan horses." In contrast, our knowledge of the mechanisms by which extracellular bacterial pathogens enter the CNS remains limited. In most cases, the precise site of entry is unknown. This is explained by the paucity of animal models featuring CNS invasion after systemic inoculation and by the lack of good in vitro models of the various CNS barriers. Interest in the phenomenon of spirochetal neurological involvement dates to the early 20th century, when the incidence of syphilis and RF was much higher (8). Since the 1980s, neurological complications were described in Lyme disease (43), resulting in a renewed interest in this phenomenon. CNS infection is rare in rodent models of Lyme disease and inconsistent and short-lived in nonhuman primates, unless the animals are immunosuppressed (2, 10). In contrast, neuroborreliosis is a frequent occurrence in animal models of RF (9, 15, 24, 38). Previous studies using culture (15) and immunohistochemistry (12) showed that serotype 1 is more neurotropic than serotype 2. The present study confirmed this observation and revealed an important association between serotype 1 and endothelial cells in the cerebral microcirculation.

We confirmed in vivo that serotype 1 is significantly more neuroinvasive than serotype 2. Evidence of this included measures of both infection and inflammation (Table 1). Since the only difference between isogenic serotypes 1 and 2 is their Vsp, this provides further support to the hypothesis that a novel function of RF Vsp is modulation of the ability to enter the CNS; in other words, neuroinvasion. Cerebral microgliosis is a prominent feature of neuroborreliosis in RF in both experimental animals (35) and humans (11). The extensive cerebral microgliosis of *scid* mice persistently infected with serotype 1 could not be explained by the presence of spirochetes in the brain parenchyma. In previous studies, we found that the ratio of spirochetes in the leptomeninges to the CNS parenchyma is about 100:1 in both *scid* mice infected with *B. turicatae* (12) and immunosuppressed rhesus macaques infected with *B. burgdorferi* (2). Since *scid* mice do not produce the specific antibodies needed to clear the infection (36), we can rule out the possibility that spirochetes were cleared from the brain parenchyma. We believe it is more likely that cerebral microgliosis is an inflammatory response to the presence of spirochetes or their products in circulation, as has been reported with lipopolysaccharide from gram-negative bacteria (31). Shedding of lipoprotein-rich outer membrane vesicles has been described in vitro for Lyme disease (23) and RF (5) spirochetes, but to our knowledge it has never been proven in vivo. It is possible that if outer membrane vesicles are released from serotype 1 in the blood or cerebrospinal fluid they somehow activate brain microglia. One possibility is that these fragments cross the inflamed blood-brain barrier and enter the brain. The finding that radioactive spirochetal products can cross BMEC barriers in vitro (Fig. 7B) is supportive of this. However, it is also possible that microgliosis is a response to stimulation of the cerebral microcirculation by spirochetes in the blood and cerebrospinal fluid. Similar microgliosis has been seen in immunocompetent mice, but to a much lesser extent (14).

Several studies both in vivo and in vitro revealed there is an important interaction between *B. turicatae* and brain endothelial cells. All serotypes we tested showed significant binding to BMEC. However, the differences in neuroinvasiveness of serotype 1 and serotype 2 could not be solely be explained by differences in binding. In contrast, the studies of BMEC barrier crossing in vitro indicate that one reason serotype 1 is more neuroinvasive than serotype 2 is because it moves better across BMEC barriers. The route of entry of spirochetes from the circulation into the CNS has not been conclusively established. Studies in vitro with *T. pallidum* and *B. burgdorferi* indicate spirochetes leave the vasculature by crossing the intercellular junctions of endothelial cells (25, 48, 50). Fibronectin is involved in the binding of *B. burgdorferi* to subendothelial extracellular matrix (48). However, whether one or more of the several endothelial cell adhesion molecules upregulated by *B.*

burgdorferi, including E-selectin, vascular cell adhesion molecule 1, and intercellular adhesion molecule 1 are involved remains to be determined (46, 47). Spirochetal binding of plasminogen or other host proteases may facilitate this (17, 24, 38). However, borrelias have also been observed intracellularly in endothelial cells (33) and fibroblasts (20). Examination of the interaction of serotype 1 with BMEC by immunofluorescence showed only extracellular spirochetes. This is more consistent with crossing by a paracellular route rather than transcytosis across BMEC cytoplasm. However, we could not rule out the possibility that spirochetal proteins, like Vsp1, enter BMEC (Fig. 3).

In vitro serotype 1 associated with BMEC significantly more than with fibroblasts or arachnoidal cells. This association is likely to involve protein-protein interactions between the outer membrane of *B. turicatae* and BMEC cytoplasmic membranes. The finding that Vsp1 colocalizes with BMEC membranes by double immunofluorescence microscopy supports a role for Vsp1 in this association (Fig. 3). The complete elimination of the association by proteinase K pretreatment of BMEC supports the involvement of cell surface BMEC proteins in this association. Little is known about the components of spirochetes necessary for crossing the blood-brain barrier. Several spirochetal proteins that bind to eukaryotic cells have been reported. These include VMPs of RF borrelias (49) and outer surface proteins (45) and decorin-binding proteins (27) of LD borrelias. Similarly, several eukaryotic cell adhesion molecules for spirochetes have been identified, including integrins (16), glycolipids (21), proteoglycans (28), and glycosaminoglycans (32). Vsp1 and Vsp2 of *B. turicatae* have been found to have some affinity for glycosaminoglycans, although the overall binding is low (34). One group reported eukaryotic cell adhesion molecules increases in venular endothelial cells upon exposure to Lyme disease borrelias (47). However, whether this occurs in the cerebral microcirculation is not known. To our knowledge, no eukaryotic cell proteins involved in binding of spirochetes to the cerebral microcirculation have been described.

These studies provide novel information regarding the interaction of a neurotropic spirochete with the cerebral microcirculation. Binding to brain endothelial cells appears to be important but not sufficient to explain the differences in neuroinvasiveness of isogenic serotypes of *B. turicatae*. The reason for the extensive cerebral microgliosis in the absence of brain parenchymal spirochetes also remains unexplained. Future studies in vivo using infectious recombinant borrelias and the identification of cell surface proteins involved in the interaction of BMEC with *B. turicatae* will be helpful to better understand the phenomenon of neuroinvasiveness of spirochetes.

ACKNOWLEDGMENTS

This work was supported by grants from the Foundation of UMDNJ and Scientist Development Grant 0235464T from the American Heart Association to D.C.

We thank Robert Martuza from Harvard University for his gift of the F5 meningioma cell line, Wolfram R. Zückert from the University of Kansas Medical Center for valuable discussions, and Joan Skurnick from UMDNJ-New Jersey Medical School for assistance with the statistical analysis.

REFERENCES

1. **Alugupalli, K. R., R. M. Gerstein, J. Chen, E. Szomolanyi-Tsuda, R. T. Woodland, and J. M. Leong.** 2003. The resolution of relapsing fever borreliosis requires IgM and is concurrent with expansion of B1b lymphocytes. J. Immunol. **170:**3819–3827.
2. **Bai, Y., K. Narayan, D. Dail, M. Sondey, E. Hodzic, S. W. Barthold, A. R. Pachner, and D. Cadavid.** 2004. Spinal cord involvement in the nonhuman primate model of Lyme disease. Lab. Investig. **84:**160–172.
3. **Barbour, A., S. Tessier, and H. Stoenner.** 1982. Variable major proteins of Borrelia hermsii. J. Exp. Med. **156:**1312–1324.
4. **Barbour, A. G., and S. F. Hayes.** 1986. Biology of Borrelia species. Microbiol. Rev. **50:**381–400.
5. **Barbour, A. G., W. J. Todd, and H. G. Stoenner.** 1982. Action of penicillin on *Borrelia hermsii*. Antimicrob. Agents Chemother. **21:**823–829.
6. **Cadavid, D.** 2004. Lyme disease and relapsing fever, p. 659–690. *In* W. Scheld, R. Whitley, and C. Marra (ed.), Infections of the central nervous system. Lippincott-Raven, Philadelphia, Pa.
7. **Cadavid, D., Y. Bai, D. Dail, M. Hurd, K. Narayan, E. Hodzic, S. W. Barthold, and A. R. Pachner.** 2003. Infection and inflammation in skeletal muscle from nonhuman primates infected with different genospecies of the Lyme disease spirochete *Borrelia burgdorferi*. Infect. Immun. **71:**7087–7098.
8. **Cadavid, D., and A. G. Barbour.** 1998. Neuroborreliosis during relapsing fever: review of the clinical manifestations, pathology, and treatment of infections in humans and experimental animals. Clin. Infect. Dis. **26:**151–164.
9. **Cadavid, D., V. Bundoc, and A. G. Barbour.** 1993. Experimental infection of the mouse brain by a relapsing fever Borrelia species: a molecular analysis. J. Infect. Dis. **168:**143–151.
10. **Cadavid, D., T. O'Neill, H. Schaefer, and A. R. Pachner.** 2000. Localization of Borrelia burgdorferi in the nervous system and other organs in a nonhuman primate model of lyme disease. Lab. Investig. **80:**1043–1054.
11. **Cadavid, D., and A. R. Pachner.** 2000. Neurosyphilis. *In* R. C. Griggs and R. J. Joynt (ed.), Clinical neurology on CD ROM. Lippincott-Raven, Philadelphia, Pa.
12. **Cadavid, D., A. R. Pachner, L. Estanislao, R. Patalapati, and A. G. Barbour.** 2001. Isogenic serotypes of *Borrelia turicatae* show different localization in the brain and skin of mice. Infect. Immun. **69:**3389–3397.
13. **Cadavid, D., P. M. Pennington, T. A. Kerentseva, S. Bergstrom, and A. G. Barbour.** 1997. Immunologic and genetic analyses of VmpA of a neurotropic strain of *Borrelia turicatae*. Infect. Immun. **65:**3352–3360.
14. **Cadavid, D., M. Sondey, E. Garcia, and C. L. Lawson.** 2006. Residual brain infection in relapsing fever borreliosis. J. Infect. Dis. **193:**1451–1458.
15. **Cadavid, D., D. D. Thomas, R. Crawley, and A. G. Barbour.** 1994. Variability of a bacterial surface protein and disease expression in a possible mouse model of systemic Lyme borreliosis. J. Exp. Med. **179:**631–642.
16. **Coburn, J., J. M. Leong, and J. K. Erban.** 1993. Integrin alpha IIb beta 3 mediates binding of the Lyme disease agent Borrelia burgdorferi to human platelets. Proc. Natl. Acad. Sci. USA **90:**7059–7063.
17. **Coleman, J. L., T. J. Sellati, J. E. Testa, R. R. Kew, M. B. Furie, and J. L. Benach.** 1995. *Borrelia burgdorferi* binds plasminogen, resulting in enhanced penetration of endothelial monolayers. Infect. Immun. **63:**2478–2484.
18. **Comstock, L. E., and D. D. Thomas.** 1991. Characterization of Borrelia burgdorferi invasion of cultured endothelial cells. Microb. Pathog. **10:**137–148.
19. **Connolly, S. E., D. G. Thanassi, and J. L. Benach.** 2004. Generation of a complement-independent bactericidal IgM against a relapsing fever borrelia. J. Immunol. **172:**1191–1197.
20. **Franz, J. K., O. Fritze, M. Rittig, G. Keysser, S. Priem, J. Zacher, G. R. Burmester, and A. Krause.** 2001. Insights from a novel three-dimensional in vitro model of lyme arthritis: standardized analysis of cellular and molecular interactions between Borrelia burgdorferi and synovial explants and fibroblasts. Arthritis Rheum. **44:**151–162.
21. **Garcia-Monco, J. C., B. Fernandez Villar, R. C. Rogers, A. Szczepanski, C. M. Wheeler, and J. L. Benach.** 1992. Borrelia burgdorferi and other related spirochetes bind to galactocerebroside. Neurology **42:**1341–1348.
22. **Garcia-Monco, J. C., B. F. Villar, J. C. Alen, and J. L. Benach.** 1990. Borrelia burgdorferi in the central nervous system: experimental and clinical evidence for early invasion. J. Infect. Dis. **161:**1187–1193.
23. **Garon, C. F., D. W. Dorward, and M. D. Corwin.** 1989. Structural features of Borrelia burgdorferi–the Lyme disease spirochete: silver staining for nucleic acids. Scanning Microsc. Suppl. **3:**109–115.
24. **Gebbia, J. A., J. C. Monco, J. L. Degen, T. H. Bugge, and J. L. Benach.** 1999. The plasminogen activation system enhances brain and heart invasion in murine relapsing fever borreliosis. J. Clin. Investig. **103:**81–87.
25. **Grab, D. J., G. Perides, J. S. Dumler, K. J. Kim, J. Park, Y. V. Kim, O. Nikolskaia, K. S. Choi, M. F. Stins, and K. S. Kim.** 2005. Borrelia burgdorferi, host-derived proteases, and the blood-brain barrier. Infect. Immun. **73:**1014–1022.
26. **Graham, D., and P. Lantos.** 1997. Greenfield's neuropathology, 6th ed., vol. 1. Oxford University Press, New York, N.Y.
27. **Guo, B. P., E. L. Brown, D. W. Dorward, L. C. Rosenberg, and M. Hook.**

1998. Decorin-binding adhesins from Borrelia burgdorferi. Mol. Microbiol. **30:**711–723.
28. **Guo, B. P., S. J. Norris, L. C. Rosenberg, and M. Hook.** 1995. Adherence of *Borrelia burgdorferi* to the proteoglycan decorin. Infect. Immun. **63:**3467–3472.
29. **Hara, H., K. D. Lamon, and H. Kaji.** 1981. Effect of temperature on normal and SV40-transformed human fibroblasts. Biochim. Biophys. Acta **673:** 37–45.
30. **Hirschfeld, M., C. J. Kirschning, R. Schwandner, H. Wesche, J. H. Weis, R. M. Wooten, and J. J. Weis.** 1999. Cutting edge: inflammatory signaling by Borrelia burgdorferi lipoproteins is mediated by toll-like receptor 2. J. Immunol. **163:**2382–2386.
31. **Lacroix, S., D. Feinstein, and S. Rivest.** 1998. The bacterial endotoxin lipopolysaccharide has the ability to target the brain in upregulating its membrane CD14 receptor within specific cellular populations. Brain Pathol. **8:**625–640.
32. **Leong, J. M., P. E. Morrissey, E. Ortega-Barria, M. E. Pereira, and J. Coburn.** 1995. Hemagglutination and proteoglycan binding by the Lyme disease spirochete, *Borrelia burgdorferi*. Infect. Immun. **63:**874–883.
33. **Ma, Y., A. Sturrock, and J. J. Weis.** 1991. Intracellular localization of *Borrelia burgdorferi* within human endothelial cells. Infect. Immun. **59:**671–678.
34. **Magoun, L., W. R. Zuckert, D. Robbins, N. Parveen, K. R. Alugupalli, T. G. Schwan, A. G. Barbour, and J. M. Leong.** 2000. Variable small protein (Vsp)-dependent and Vsp-independent pathways for glycosaminoglycan recognition by relapsing fever spirochaetes. Mol. Microbiol. **36:**886–897.
35. **Martinez-Baez, M., and A. Villasana.** 1945. Sobre la histopatologia de la fiebre recurrente experimental. Rev. Inst. Salubr. Enferm. Trop. **6:**185–194.
36. **Newman, K., Jr., and R. C. Johnson.** 1984. T-cell-independent elimination of *Borrelia turicatae*. Infect. Immun. **45**:572–576.
37. **Nizet, V., K. S. Kim, M. Stins, M. Jonas, E. Y. Chi, D. Nguyen, and C. E. Rubens.** 1997. Invasion of brain microvascular endothelial cells by group B streptococci. Infect. Immun. **65:**5074–5081.
38. **Nordstrand, A., A. Shamaei-Tousi, A. Ny, and S. Bergstrom.** 2001. Delayed invasion of the kidney and brain by *Borrelia crocidurae* in plasminogen-deficient mice. Infect. Immun. **69:**5832–5839.
39. **Pachner, A. R., D. Dail, Y. Bai, M. Sondey, L. Pak, K. Narayan, and D. Cadavid.** 2004. Genotype determines phenotype in experimental Lyme borreliosis. Ann. Neurol. **56:**361–370.
40. **Pennington, P. M., D. Cadavid, and A. G. Barbour.** 1999. Characterization of VspB of *Borrelia turicatae*, a major outer membrane protein expressed in blood and tissues of mice. Infect. Immun. **67:**4637–4645.
41. **Pennington, P. M., D. Cadavid, J. Bunikis, S. J. Norris, and A. G. Barbour.** 1999. Extensive interplasmidic duplications change the virulence phenotype of the relapsing fever agent Borrelia turicatae. Mol. Microbiol. **34:**1120–1132.
42. **Perry, V. H., D. A. Hume, and S. Gordon.** 1985. Immunohistochemical localization of macrophages and microglia in the adult and developing mouse brain. Neuroscience **15:**313–326.
43. **Reik, L., A. C. Steere, N. H. Bartenhagen, R. E. Shope, and S. E. Malawista.** 1979. Neurologic abnormalities of Lyme disease. Medicine **58:**281–294.
44. **Rock, R., G. Gekker, S. Hu, W. Shen, M. Cheeran, J. Lokensgard, and P. Peterson.** 2004. Role of microglia in central nervous system infections. Clin. Microbiol. Rev. **17:**942–964.
45. **Sadziene, A., D. D. Thomas, and A. G. Barbour.** 1995. *Borrelia burgdorferi* mutant lacking Osp: biological and immunological characterization. Infect. Immun. **63:**1573–1580.
46. **Sellati, T. J., L. D. Abrescia, J. D. Radolf, and M. B. Furie.** 1996. Outer surface lipoproteins of *Borrelia burgdorferi* activate vascular endothelium in vitro. Infect. Immun. **64:**3180–3187.
47. **Sellati, T. J., M. J. Burns, M. A. Ficazzola, and M. B. Furie.** 1995. *Borrelia burgdorferi* upregulates expression of adhesion molecules on endothelial cells and promotes transendothelial migration of neutrophils in vitro. Infect. Immun. **63:**4439–4447.
48. **Szczepanski, A., M. B. Furie, J. L. Benach, B. P. Lane, and H. B. Fleit.** 1990. Interaction between Borrelia burgdorferi and endothelium in vitro. J. Clin. Investig. **85:**1637–1647.
49. **Thomas, D., D. Cadavid, and A. Barbour.** 1994. Differential association of Borrelia species with cultured neural cells. J. Infect. Dis. **169:**445–448.
50. **Thomas, D., M. Navab, D. Haake, A. Fogelman, J. Miller, and M. Lovett.** 1988. Treponema pallidum invades intercellular junctions of endothelial cell monolayers. Proc. Natl. Acad. Sci. USA **85:**3608–3612.

Editor: J. B. Bliska